




Ion Channels in Critical Membranes: Clustering, Cooperativity, and Memory Effects

Antonio Suma ^{1,2,*} Daniel Sigg ^{2,3} Seamus Gallagher,² Giuseppe Gonnella,¹ and Vincenzo Carnevale ^{2,†}

¹*Dipartimento di Fisica, Università degli Studi di Bari and INFN, Sezione di Bari, via Amendola 173, Bari I-70126, Italy*

²*Institute for Computational Molecular Science, Temple University, Philadelphia, Pennsylvania 19122, USA*

³*dPET, Spokane, Washington 99223, USA*



(Received 14 June 2023; accepted 10 January 2024; published 8 February 2024)

Much progress has been made in elucidating the inner workings of voltage-gated ion channels, but less understood is the influence of lipid rafts on gating kinetics. Here we propose that state-dependent channel affinity for different lipid species provides a unified explanation for the experimentally observed behaviors of clustering, cooperativity, and hysteresis. We develop models of diffusing lipids and channels engaged in Ising-like interactions to investigate the collective behaviors driven by raft formation in critical membranes close to the demixing transition. The model channels demonstrate lipid-mediated long-range interactions, activation curve steepening, and long-term memory in ionic currents. These behaviors likely play a role in channel-mediated cellular signaling and suggest a universal mechanism for self-organization of biomolecular assemblies.

DOI: [10.1103/PRXLife.2.013007](https://doi.org/10.1103/PRXLife.2.013007)

I. INTRODUCTION

Ion channels play a critical and ubiquitous role in cellular signaling by transmuting external forces into changes in ion permeability across membranes, a process known as gating. The discovery of on/off ionic currents catalyzed by a single pore [1,2] led to a reinterpretation of the seminal Hodgkin and Huxley equations [3] as stochastic gating by independent channels [4]. As electrophysiological and biochemical techniques improved, gating schemes expanded to accommodate new data [5,6], but the assumption that channels gate independently has persisted.

The paradigm of the independent channel has been challenged by experiments that directly visualize the cellular membrane, such as electron microscopy, confocal fluorescence microscopy, and superresolution imaging [7–10]. Channels are seen to aggregate in clusters ranging in size from a few channels to large groups containing tens of thousands of channels. Factors that contribute to clustering include direct channel-channel interactions [11] and connections to the cytoskeleton [12].

Here we consider another mechanism of clustering that is mediated by the lipid membrane. The fluidlike dynamics of a heterogeneous population of lipids can indirectly mediate channel interactions. The notion that conformational changes in the channel can affect and be affected by the thermodynamic properties of the membrane is supported by a range of evidence from cryoEM, electrophysiology, and computa-

tional studies [13–23]. Lipid membranes under physiological conditions are close to the demixing transition, resulting in the formation of rafts and liquid disordered domains [24–27]. Near the critical temperature, membranes are subject to fluctuations in local composition characterized by large correlation lengths [28].

Membrane demixing can explain two observations that are currently poorly understood: (i) the unusual size distribution of clusters of ion channels, which can follow a power-law behavior, see Supplemental Material (SM) [29] analysis from Ref. [8], and (ii) the long-term memory effects seen in single-channel recordings [30–35]. Furthermore, since interactions with specific lipid species have been shown to selectively stabilize the open or closed state of the pore [36], near-critical long-range lipid interactions offer explanations for other anomalous channel behaviors, such as enhanced cooperativity [11,37], modal gating [38–40], and hysteresis [41–43].

In this work we propose a unified explanation for the size distribution of clusters and gating anomalies based on the assumption that distinct conformational states of the channel (including open and closed) have affinities for different lipids species. To this end we introduce two complementary phenomenological descriptions of ion channels embedded in a lipid mixture: (i) a mesoscopic model of lipid membranes that faithfully describes the membrane phase behavior and its coupling to the channel conformation; and (ii) a discrete-state Markov model of interacting channel-lipid systems with a realistic description of channel gating kinetics. The first model is a minimalist representation of lipids and channels whose purpose is to demonstrate that these collective phenomena are independent of any specific molecular detail but rather derive from the combination of state-dependent interactions and critical demixing. The second model builds on a more realistic representation of the channel structure and activation dynamics and allows us to ascertain that the effects investigated here occur on physiologically relevant length- and timescales. In both models, we find that fluctuations in the underlying lipid

*Corresponding author: antonio.suma@uniba.it

†Corresponding author: vincenzo.carnevale@temple.edu

Published by the American Physical Society under the terms of the Creative Commons Attribution 4.0 International license. Further distribution of this work must maintain attribution to the author(s) and the published article's title, journal citation, and DOI.

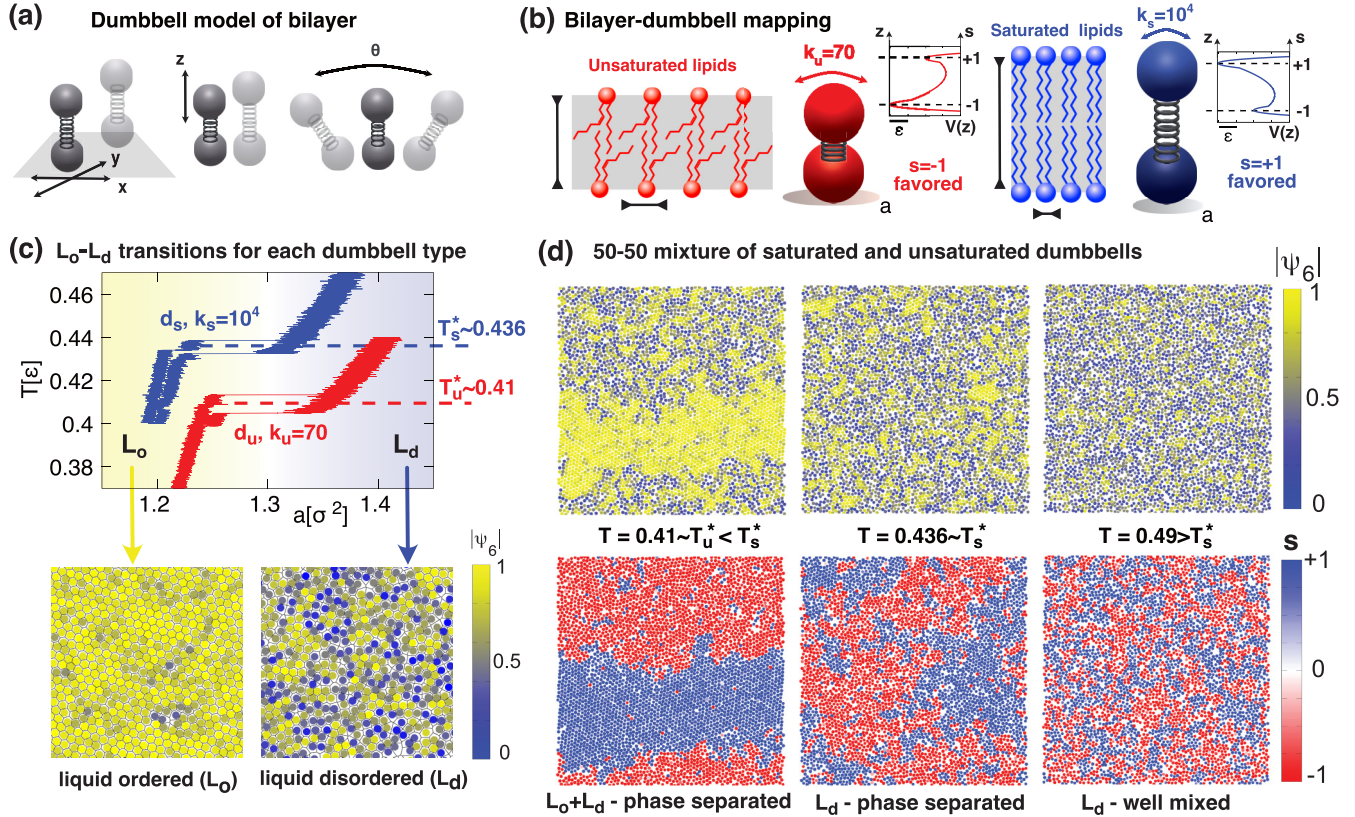


FIG. 1. (a) Mesoscopic model of lipids, represented by a dumbbell which can diffuse on the xy plane (bottom bead constrained in plane), has a varying z height of top bead, and a deviation (θ angle) from the vertical orientation restrained by a harmonic potential of force constant k (SM [29]). (b) Bilayer-dumbbell mapping. Unsaturated (saturated) lipids are mapped onto d_u (d_s) dumbbells, with a global minimum of the height potential [see $V(z)$] corresponding to short (long) dumbbell or spin $s = -1$ ($+1$), and a small (large) tilting constant, $k_u = 70$ ($k_s = 10^4$), which entails a large (small) surface area a . (c) Plots of temperature vs a for d_u and d_s , obtained via heating or cooling the system (two curves for each type). Both dumbbell types exhibit a liquid-ordered (L_o , associated to hexatic ordering) to liquid-disordered (L_d) phase transition; see snapshots colored with local hexatic modulus $|\psi_6|$ (SM [29]). As curves do not coincide due to hysteresis [17], ordering from the disordered phase is much slower than disordering from the ordered phase, we considered as transition temperature the average value in between the heating or cooling curves plateau, $T_u^* \sim 0.41$ and $T_s^* \sim 0.436$. The melting temperature is shifted towards higher T as k is increased. (d) 50-50 mixture of d_u and d_s dumbbells at three temperatures, $T = 0.41, 0.436, 0.49$. Each column shows an equilibrated conformation for the indicated temperature, colored by the hexatic modulus and spin value (top and bottom row, respectively).

medium give rise to long-range effective attractive forces, leading to clustering, cooperative gating, hysteresis, and long-memory effects in the channel gating dynamics.

II. RESULTS

A. A mesoscopic model of ion channels in phase-separating membranes

To study the dynamics of channels embedded in a lipid bilayer, we introduce a simplified mesoscale representation of the membrane and of the embedded ion channels.

The membrane is described by an assembly of molecules of two types, each representing saturated or unsaturated lipids. The assembly is meant to mimic the phase behavior of a three-component membrane in physiological conditions [44,45]. In cholesterol-containing ternary mixtures with saturated and unsaturated lipids, saturated lipids tend to segregate into liquid ordered (L_o) domains, while unsaturated lipids promote the formation of a liquid disordered phase (L_d). L_o domains are characterized by hexatic order (see [17,27,46,47] and SM [29]

for a definition) and a larger membrane thickness compared to the L_d phase, see Fig. 1(b). At fixed temperature, the transition from a well-mixed liquid disordered membrane to a phase-separated coexistence of L_o and L_d domains is driven by a change in lipid composition (i.e., a change in the cholesterol and lipids molar fractions). Importantly, at fixed composition, this mixing-demixing transition can be driven by a change in temperature: higher temperatures promote mixing of the two lipids into a liquid disordered (L_d) phase.

We model each ion channel as a multidomain inclusion in the membrane in which each domain is allowed to fluctuate across a single-barrier conformational landscape. The stable basins are meant to recapitulate the two-state character of ion channels that cycle through open or closed (in the case of the central pore unit) and resting or activated (in the case of ancillary sensory domain) conformations. We further assume that the open and closed or activated and resting conformations have affinity for saturated and unsaturated lipids, respectively. This feature of the model is meant to mimic the dependence of ion-channel activation on the properties of the embedding

membrane: this has been observed for KvAP channels, which have been shown to respond to the membrane potential differently if immersed in a bilayer of saturated or unsaturated lipids [36], and for the Eag Kv channel, whose activation entails a disorder-order transition in the surrounding lipid membrane [22]. These observations raise the intriguing possibility that local lipid composition (i.e., the ratio between saturated and unsaturated lipids) and degree of orientational order (i.e., L_o vs L_d) can potentially affect the activation properties of channels.

We built a model for the lipid bilayer by extending the particle-based Ising model described in Ref. [48], Fig. 1(a), and the SM [29]. In the particle-based Ising, basic building blocks are connected pairs of beads (i.e. a dumbbell) orthogonally oriented with respect to the membrane plane. The bottom beads are constrained to lay on the plane and interact only through a volume exclusion short-range repulsion, while the top beads interact via a Lennard-Jones potential (i.e., it also includes an attractive tail). The z position of the top bead can assume two values (the two minima of a quartic potential); we showed in Ref. [48] that these two top-bead heights can be mapped to the spin values -1 and $+1$, and the dumbbells, fixed in a triangular lattice, have a ferromagnetic-paramagnetic transition varying the temperature. This work extends the previous model by allowing dumbbells to freely diffuse (xy directions), and the dumbbell vertical orientation (described by the tilting angle θ) can vary as well through a harmonic potential with force constant k (SM [29]). All physical quantities referring to this model are expressed in Lennard-Jones units of mass m , energy ϵ , and length σ .

Considering the fact that unsaturated lipids form thinner membranes and occupy on average a larger area per lipid than saturated lipids, we modeled the former by “unsaturated” dumbbells (d_u) which occupy preferentially the $s = -1$ spin state and have a small force constant $k_u = 70$, and the latter by “saturated” dumbbells (d_s) which occupy preferentially the $s = +1$ state and have a larger value of $k_s = 10^4$ [Fig. 1(b)]. Each dumbbell type thus has a typical height, although both the $s = -1$ and $s = +1$ states are accessible and occasionally populated by all dumbbells. At any fixed temperature, constant pressure molecular dynamics simulations of single-type dumbbells show that due to the different values of k , d_u occupy on average a larger area a compared to d_s [Fig. 1(c)]. Importantly, both d_u and d_s show a transition between the L_o and L_d phase at a critical temperature T^* [Fig. 1(c), top panel], where these phases are characterized by bottom beads being hexatically ordered or disordered, respectively [Fig. 1(c), bottom panels]. d_u present a transition at $T_u^* \sim 0.41$ and d_s at $T_s^* \sim 0.436$.

When d_s and d_u are simulated together in a 50-50 mixture, we have the additional tendency of dumbbells of the same height to interact more strongly and thus to segregate. This effect depends on the dumbbells height fluctuation and thus is expected to be temperature dependent. In general, within the d_s - d_u mixture, we have a nontrivial combination of the demixing tendency and the L_o/L_d phase transition occurring for each dumbbell type [Fig. 1(d)]. Our choice of parameters led to a behavior which is consistent with that of ternary mixtures. We find, in fact, that for $T = 0.41 \sim T_u^* < T_s^*$, the two dumbbell types demix, with d_s forming a high-density, hexatically ordered phase, identified as L_o domains, while d_u

form a disordered (L_d) phase. For $T = 0.436 \sim T_s^*$, we still observe a nearly phase-separated system where mixing starts to occur but clusters still fluctuate in size, and both phases are disordered (L_d). These fluctuations are large, as expected for binary mixture near the demixing transition [49]. For $T = 0.49 > T_s^*$ we have a completely mixed and disordered phase (L_d).

We now introduce a simplified representation of ion channels to model the observation that each distinct configuration (open or closed) interacts preferentially with a specific lipid species. The goal is to understand how the coupling between the internal degrees of freedom of the channel and those of the lipids can give rise to the collective phenomena mentioned in the Introduction. Our goal is to introduce a simple nontrivial model representing a voltage-gated ion channel. A single dumbbell has only two accessible states, up and down, while a collection of dumbbells increases the combinatorial landscape. The presence of multiple states makes it possible to study cooperativity as an enhanced two-state character of the system.

The channel is a collection of dumbbells arranged in a hexagonal shape, with coplanar neighboring beads connected via springs [Fig. 2(a)]. This shape does not perturb the hexatic order of dumbbells and gives a sufficiently large interaction surface with lipids. The z coordinate of top beads is subjected to an external bias force, F_p , mimicking the membrane potential. Top beads move on z in a two-well potential, with equally probable states without external bias ($F_p = 0$) and with a smaller barrier than lipid dumbbells, to facilitate transitions between the two states. When biased, one state becomes more populated than the other. By assigning the role of “pore domain” to the central dumbbell, we define a proxy for the two conductance states, closed and open, based on the dumbbell spin state. Accordingly, the remaining six dumbbells can be interpreted as voltage sensor domains. Importantly, due to the attractive Lennard-Jones potential, each channel state interacts preferentially with lipid species having the same height (or spin state). Channels interact with one another or with lipids via the same potential (SM [29]).

We first look at the channel-channel clustering tendency due to lipid-mediated interactions and the resulting segregation effects. We then turn our attention to cooperativity and dynamical and out-of-equilibrium effects.

1. Lipid-mediated interactions

Figure 2(b) demonstrates the effect of channels within a membrane at the three temperatures considered ($T = 0.41, 0.436, 0.49$) with a fixed channels-to-lipids ratio of $f_p = 0.05$ (from now on we refer to d_s and d_u dumbbells as lipids). The top row shows the effect without an applied external potential on the channels, $F_p = 0$, while the bottom row shows the effect with $F_p = 1$.

Comparing the first row of Fig. 2(b) to Fig. 1(d), we see that channels promote lipid mixing at $T = 0.41$ and $F_p = 0$, in the sense that the L_d and L_o interface margins are less well defined. This can be explained by the fact that unbiased channels can act as lineactants between the two phases [50]. On the other hand, the lipid-channel attraction strength is the same as for channel-channel, and thus channels remain in a diluted state. Across all temperatures, unbiased channels can

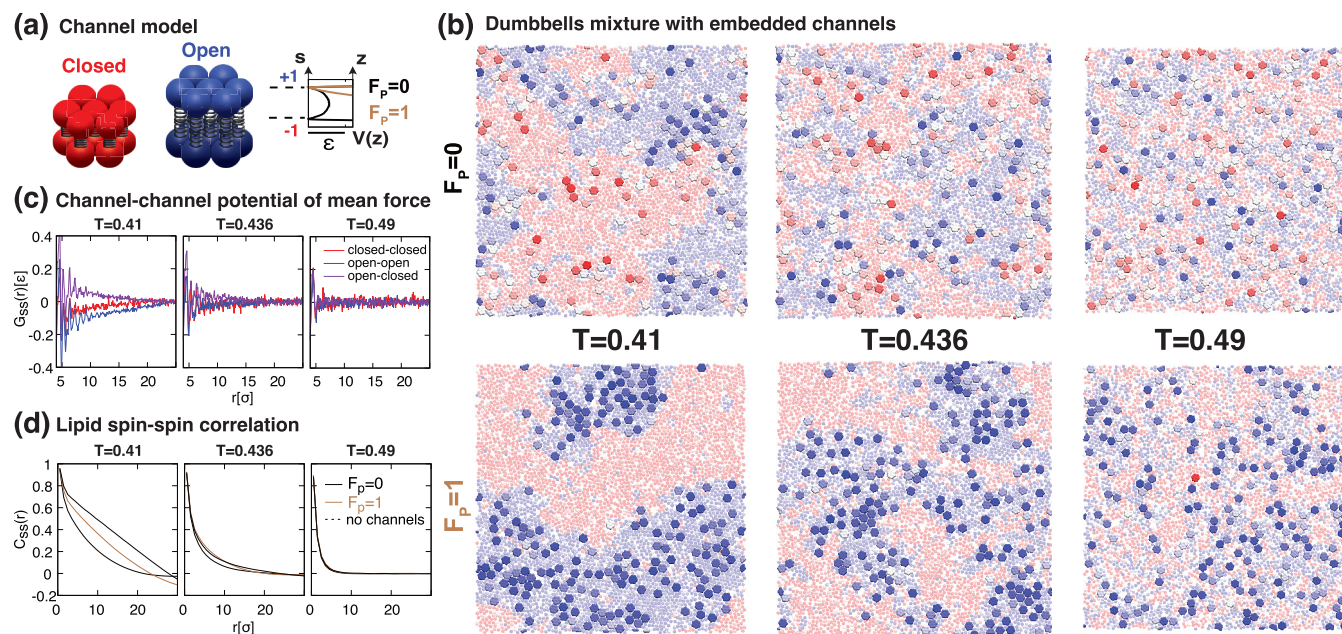


FIG. 2. (a) Mesoscopic model of ion channel, with seven dumbbells assembled in a hexagonal shape and coplanar neighbor beads connected via springs (SM [29]). Top beads are subject to an external field F_p in the z direction, which models the membrane potential. Average top bead height fluctuates around two equally probable states when $F_p = 0$, while one of the two states becomes favored when $F_p \neq 0$ (see potential $V(z)$ of z , the average channel top bead height). The central dumbbell has the role of the pore, with its spin mapped to a closed-open state. (b) Snapshots of embedded channels (darker colors) in the binary dumbbell mixture of Fig. 1(d), at three temperatures ($T = 0.41, 0.436, 0.49$) and $F_p = 0, 1$ (top and bottom row). Channel-lipid ratio is $f_p = 0.05$, and dumbbells are colored according to their spin value [color scheme in Fig. 1(d)]. (c) Potential of mean force as a function of distance between two channel pores in the open-open, closed-closed, and open-closed configuration, same T as in (b) and $F_p = 0$. (d) Lipids spin-spin correlation with embedded channels and compared to lipid-only mixture, for the cases shown in (b).

diffuse into both lipid phases and tend to assume their height or spin state.

When an external field is applied to channels, they are biased towards one or the other spin state based on the direction of the force [Fig. 2(a)], assuming either an open or closed conformation. In the case of Fig. 2(b), we apply a force of $F_p = 1$, which biases the channels to adopt the spin-up (open) conformation. At equilibrium, channels migrate towards the phase with the same height, which in this case is the phase with spin-up lipids. As a result, channels effectively behave like lipids of the same height, causing the system to become more similar to one made up of only lipids [compare second row of Fig. 2(b) to that of Fig. 1(d)].

Of particular interest is the determination of whether channels show an attraction or repulsion between each other, due exclusively to the fact that channels are immersed in lipids with the same or opposite spin. To investigate this effect, we calculated the potential of mean force between channels when they are both open or both closed and when one is open and the other one is closed [Fig. 2(c)]. The potential of mean force is computed as $G_{ss}(r) = -k_B T \ln P_{ss}(r)$, with $P_{ss}(r)$ being the probability of having two channel pores with spin values ss at distance r . We find that channels in the same conformation display long-range lipid-mediated attraction, which is stronger near the demixing transition and decreases as the lipids begin to mix. Moreover, channels in the open conforma-

tion will feel a stronger attraction than channels in the closed conformation. In contrast, channels in different conformations show long-range lipid-mediated repulsion. These effects can be understood by considering that channels in the same phase are constrained to have the same conformation, regardless of their distance. Open channels are embedded in a denser environment and, as a result, lipid-mediated interactions are stronger. The range of the potential of mean force reflects the typical size of the underlying lipid patches. Note that the existence of these lipid-mediated long-range interactions occurring under critical conditions (known as Casimir forces) was already predicted theoretically [15,51] and shown in atomistic simulations [17,51].

Conversely, the effect of channels on the lipid patch can be understood by considering the lipid-lipid spin-correlation function [Fig. 2(d)], defined as $C_{ss}(r) = \langle s_i s_j \rangle$, with s_i the spin assigned to each lipid and r the distance between two lipids. At $F_p = 0$ and temperatures near the demixing, the function decays much faster than the corresponding decay calculated for systems without channels (dashed line), while at $F_p = 1$ the correlation becomes longer. The longer-range correlation for $F_p = 1$ is a consequence of the fact that channels are all in the same state and thus attract same-height lipids around them, locally increasing the lipid spin-spin correlation. Conversely, at $F_p = 0$ channels are free to fluctuate between the two states and adapt to the local environment. This lineactantlike

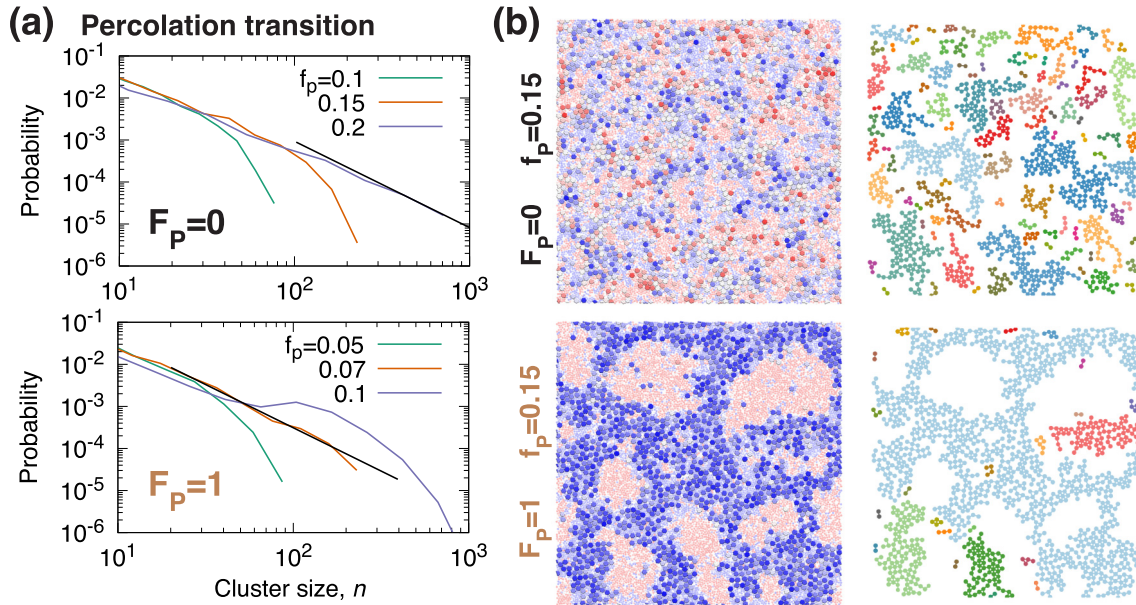


FIG. 3. (a) Cluster size distributions at $T = 0.436$, $F_p = 0, 1$, and different channel concentrations f_p . Upon increasing f_p , the distribution changes from a power law with an exponential cutoff, to a pure power law at the percolation transition, to a single peak (not shown). The critical density decreases from $f_p \sim 0.2$ at $F_p = 0$ to ~ 0.07 at $F_p = 1$. (b) First column: Spin-colored snapshots of system with $f_p = 0.15$, $T = 0.436$, at $F_p = 0, 1$ (top and bottom row). Second column: same system configurations, showing only the pore dumbbells colored according to the cluster's label. Despite the fact that f_p is the same, at $F_p = 1$ channels are more interconnected than at $F_p = 0$, as they are pushed in the spin-up phase.

behavior causes a roughening of the domain boundaries and thus a decrease in lipid spin-spin correlation.

2. Percolation transition

We now turn our attention to the effects of channel density on the system, Fig. 3, fixing $T = 0.436$. At $F_p = 0$ and for small values of f_p , we observe that the size distribution of channel clusters has the typical shape of a power law with exponential cut-off correction, $P(n) \sim n^{-\tau} e^{-n/n^*}$, with n^* a typical cluster size [Fig. 3(a), first row]. By increasing the channel density, the distribution first tends to a pure power law for $f_p \sim 0.2$, $P(n) \sim n^{-\tau}$, and then it develops a peak at large n (not shown). This behavior is in general associated with a percolation transition [52], which in two dimensions is characterized by the critical Fisher exponent $\tau = 187/91$. Notably, the same exponent is observed in the experiments shown in Fig. S1 from Ref. [8].

An interesting role in this percolation transition is played by the external field F_p [Fig. 3(a), second row]. When applied, the field shifts the transition towards lower densities, $f_p \sim 0.07$. The reason is that, when activated, channels are encouraged to migrate to the most favorable lipid phase. In this way, the surface area occupied by channels decreases (by a factor of 2) and, accordingly, the effective density increases [Fig. 3(b)]. Overall, the percolation transition is observed for a smaller channel-lipid ratio.

3. Channel-channel coupling and cooperativity

We now investigate whether the presence of lipid-mediated interactions has any effect on the ion-channel response to the trans-membrane potential. Experimentally, this may be investigated in a voltage-clamp setting by recording the

steady-state ion current, or pore conductance G , as a function of the applied voltage V . Voltage-gated ion channels contain specialized domains (voltage sensors) that increase the voltage sensitivity of the conduction pore through allosteric coupling; this increased responsiveness to the trans-membrane potential is manifested as a steepening of the “ G - V ” curve. We expect lipid-mediated interactions between voltage sensors in the same channel and between neighboring channels to enhance the voltage sensitivity of conductance in a predictable temperature-dependent manner.

To reproduce the G - V curve, we computed the equilibrium probability P_{up} that the central “pore” particle of each seven-dumbbell channel is in a spin-up state (open conformation). The conductance is related to P_{up} through $G = NgP_{up}$, where N is the number of channels and g is the single-pore conductance (assumed constant). We simulated a normalized G - V curve by calculating P_{up} as a function of the bias force F_p , as shown in Fig. 4(a), where we compare these curves in the case of an isolated (bare) channel, and of a channel embedded in the lipid bilayer, for three different temperatures. As anticipated, we notice a temperature dependence, which is stronger in the case of embedded channels.

However, one must distinguish between the effect due to a trivial temperature dependence of Boltzmann weights and the temperature dependence that arises from subtle modulations of intra- and interchannel interactions. To discriminate between these two effects, we considered the “conductance” Hill plot, which eliminates the trivial T dependence by reporting on the free energy of pore activation $W = k_B T \log[P_{up}/(1 - P_{up})]$ as a function of the external field [53]. In particular, we are interested in the vertical separation ΔW between the two linear asymptotic trends observed at extreme field

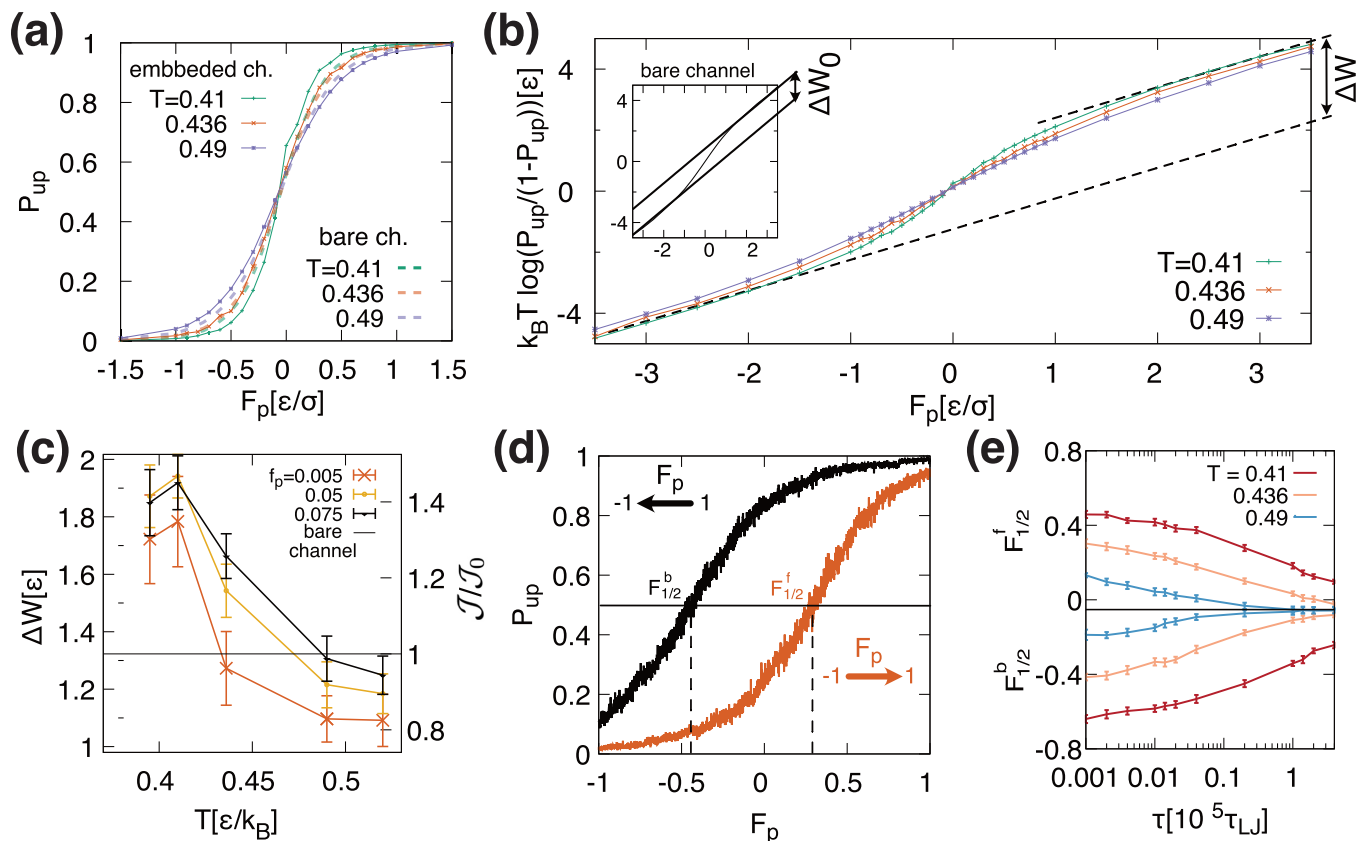


FIG. 4. (a) Probability that the pore dumbbell of a channel, embedded in the lipid bilayer, is in the up-state (P_{up}) as a function of the external field F_p , for different temperatures, at $f_p = 0.05$ (continuous lines). For comparison, the same curves for a bare channels are plotted (dashed lines) at the same temperatures. These are shifted on the F_p axis so that the values at $P_{up} = 0.5$ coincide with those of the embedded channels. (b) Hill plot of the same data shown in (a). The pore linkage energy, ΔW , defined as the vertical separation between the Hill's plot asymptotes, decreases upon increasing the temperature. In the inset, the Hill plot for a bare channel is shown. (c) ΔW as a function of temperature for three different densities f_p . The horizontal line shows the temperature-independent reference value ΔW_0 of the bare channel. (d) Activation curves at $T = 0.41$, $f_p = 0.05$ obtained by ramping-up from $F_p = -1$ to 1 (forward, red), and vice versa (backward, black), in a timing interval $\tau = 2 \times 10^4 \tau_{LJ}$. Note the marked hysteresis. Field strengths required to activate half of the channels ($P_{up} = 0.5$) are indicated as $F_{1/2}^f$ and $F_{1/2}^b$ for the forward and backward processes, respectively. (e) $F_{1/2}^f$ and $F_{1/2}^b$ as a function of the ramp duration τ . Averages are performed over five independent runs.

strengths. This amounts to removing from the free energy the linear field-coupling term, thereby isolating the effective interaction energy between the pore and the voltage-sensitive particles [53]. The entire procedure eliminates the weak inverse-temperature dependence of the G - V slope intrinsic to the Boltzmann distribution, which exists even for the bare channel [Fig. 4(a)] and reveals a more interesting lipid-mediated temperature sensitivity.

An exact expression of W is found for the isolated (bare) seven-dumbbell channel, which exists as a system of connected spins with ferromagnetic coupling constant \mathcal{J}_0 between the pore and each voltage sensor (SM [29]). In this system, the coupling energy of the bare channel is found to be proportional to \mathcal{J}_0 , $\Delta W_0 = 24\mathcal{J}_0$. Embedding the channels in a lipid environment affects the coupling energy ΔW , see Fig. 4(b). This modulation of lipid-channel and channel-channel interactions can be captured by an effective, temperature-dependent coupling constant, $\mathcal{J} \equiv \Delta W/24$, which takes into account the effect of the environment and provides a quantitative measure of the system's coopera-

tivity. Increasing \mathcal{J} , and thus ΔW , steepens the closed-to-open transition, emphasizing the two-state character of the channel.

Figure 4(c) shows the fitted ΔW for different temperatures and channel densities compared to the temperature-independent value ΔW_0 for the bare channel (SM for the fitting procedure [29]). Two major observations can be made from the figure.

First, there is a crossover between \mathcal{J} and \mathcal{J}_0 around the critical temperature ($T \sim 0.436$) with $\mathcal{J} > \mathcal{J}_0$ or $\mathcal{J} < \mathcal{J}_0$ depending on whether the channel is embedded in a demixed or mixed lipid membrane. This dependence on temperature highlights the crucial role of membrane phase behavior. In the lower-temperature demixed state, channels can migrate toward the lipid patch that stabilizes the instantaneous conformational state (i.e., closed or open). This is not possible in the higher-temperature mixed state, in which the fluctuating local lipid composition gives rise to a more heterogeneous ensemble that decreases the overall two-state character of the system.

Second, higher channel densities (f_p) result in larger \mathcal{J} at a given temperature, suggesting that channels are coupled to one another and tend to activate in a cooperative fashion; the biggest gap occurs around the demixing temperature, $T \sim 0.436$. We infer that channel-channel interactions (both direct and lipid-mediated) increase cooperative gating beyond what is expected from independently gated channels. Notably, similar channel-channel gating cooperativity was found in mechanosensitive channels [54] where their attraction promotes channel closure.

4. Out-of-equilibrium effects and hysteresis

The demonstration that channel-lipid interactions enhance cooperative gating raises an interesting question: Since the response of any given channel depends crucially on the activation state of neighbor channels (and on the thermodynamic phase of the surrounding membrane), is the closed-to-open transition quasistatic or dominated by nonequilibrium effects?

To answer this question we characterized the response of channels to a time-dependent external field with a strength that increases linearly with time. Figure 4(d) illustrates P_{up} as a function of the instantaneous value of the applied F_p . The system starts at equilibrium with $F_p = -1$, and the field is gradually increased to $F_p = 1$ for a total ramp duration τ (red curve, ON ramp protocol); the black curve shows the mirror-image OFF ramp protocol. A microscopically reversible process should give rise to overlapping curves. Instead, there is definite hysteresis even for relatively long ramp times τ . Close inspection of a sample trajectory highlights the reason underlying this behavior. Inverting the polarity of the applied field results in two combined effects: It causes channels to migrate from one phase to the other, and it promotes a phase transformation in the region surrounding channels. If τ is small compared to both the typical diffusion time L^2/D (where L is the typical patch size and D is the channel diffusion constant) and the phase-separation relaxation time, then the process is out of equilibrium and hysteresis appears. To quantitatively characterize this behavior, we report the field value resulting in the activation of half of the channels, namely, $F_{1/2}$, as a function of τ for ON and OFF ramps [Fig. 4(e)]. We note that the ON and OFF protocols tend asymptotically to the same equilibrium value and that the rate of convergence is markedly temperature dependent, with hysteresis being stronger for lower temperatures.

Regarding finite-size effects, one expects that the system size imposes a cutoff on the maximum patch size encountered and in turn the latter changes the characteristic time needed for channels to cross different patches. We thus expect that dynamical properties are affected by finite-size effects more than equilibrium ones. Hysteresis, which depends on the time required for channels to migrate from one patch to the other, is indeed enhanced by considering larger systems (see SM [29]).

B. Bridging membrane physics and physiology: A lattice model

We shift gears from the molecular dynamics model that is chiefly concerned with the phase structure of the membrane to a system with more physiological relevance. Physiologists have traditionally modeled ion-channel gating kinetics using

continuous-time discrete-state Markov models [5,6]. Gating schemes with a finite number of states adequately fit macroscopic and single-channel data in response to a variety of external stimuli [55] but may be inadequate in describing types of anomalous gating explored in this paper—clustering-induced cooperativity, hysteresis, modal gating, and long-term memory. The crux of our thesis is that a complex membrane absorbs and distributes information like a field, altering the kinetics of bare channels. We thus set out to include additional degrees of freedom to the traditionally used discrete-state models to account for lipid-channel coupling. We demonstrate that this paradigm can provide a unified explanation for anomalous gating.

We consider an established kinetic model for potassium channel gating and extend it to include the effect of channel-lipid interactions. A channel system suitable for our purposes is the large-conductance calcium-activated potassium (BK) ion channel, which, under conditions of zero- or saturating calcium, is regulated by four identical voltage-sensing domains in a manner closely described by the Monod-Wyman-Changeux (MWC) model of allostery [7,56,57]. The kinetic model corresponding to an MWC scheme contains ten states [Fig 5(a)]. Each forward step corresponds to the activation of a single domain, either the pore or one of the voltage sensors. This discrete-state model results in a more realistic description of gating kinetics and a more faithful structural representation than could be achieved with the hexagonal model studied with molecular dynamics.

In order to study the effect of a dynamic lipid environment, we constructed a square-lattice system that best adapts to the fourfold symmetry of the BK channel and possesses Ising-like interactions between neighboring binary cells; see Fig. 5(b) for a schematic representation. The lattice contains channels and lipids, of which there is a 50:50 mix of two types, “saturated” and “unsaturated.” The complete lattice is large enough (128^2 cells) to contain 100 channels. An individual channel is composed of a central pore in contact with four symmetrically arranged voltage sensors, occupying a total of 20 cells. The activation of each voltage sensor corresponds to the transport across the membrane of an elementary charge q . Macroscopically, this gives rise to a current whose time integral Q is a typical measurement done in patch-clamp experiments. The response of Q to the applied voltage V is encoded by the “ Q - V ” curve. Each lipid, which occupies a single cell, is permanently fixed in the “up” or “down” state, depending on whether it represents a saturated or unsaturated species. Channels can translate and rotate, while lipids only exchange their state with neighboring lipids [right side of Fig. 5(b)], so that the saturated-unsaturated ratio is preserved. Lipids are mobile and preferentially associate with their own type via an energy penalty incurred for oppositely aligned pairs. Importantly, lipids interact with the pore and the voltage sensor in a state-dependent fashion with the same energy penalty, where unsaturated or saturated lipids preferentially bind the resting or activated states.

The model parameters were chosen to be consistent with broad stroke features of ion-channel dynamics, namely, (i) the steepness and relative positions of equilibrium gating charge (Q - V) and conductance (G - V) curves [53,58], (ii) out-of-equilibrium decay rates of these same quantities [7], and

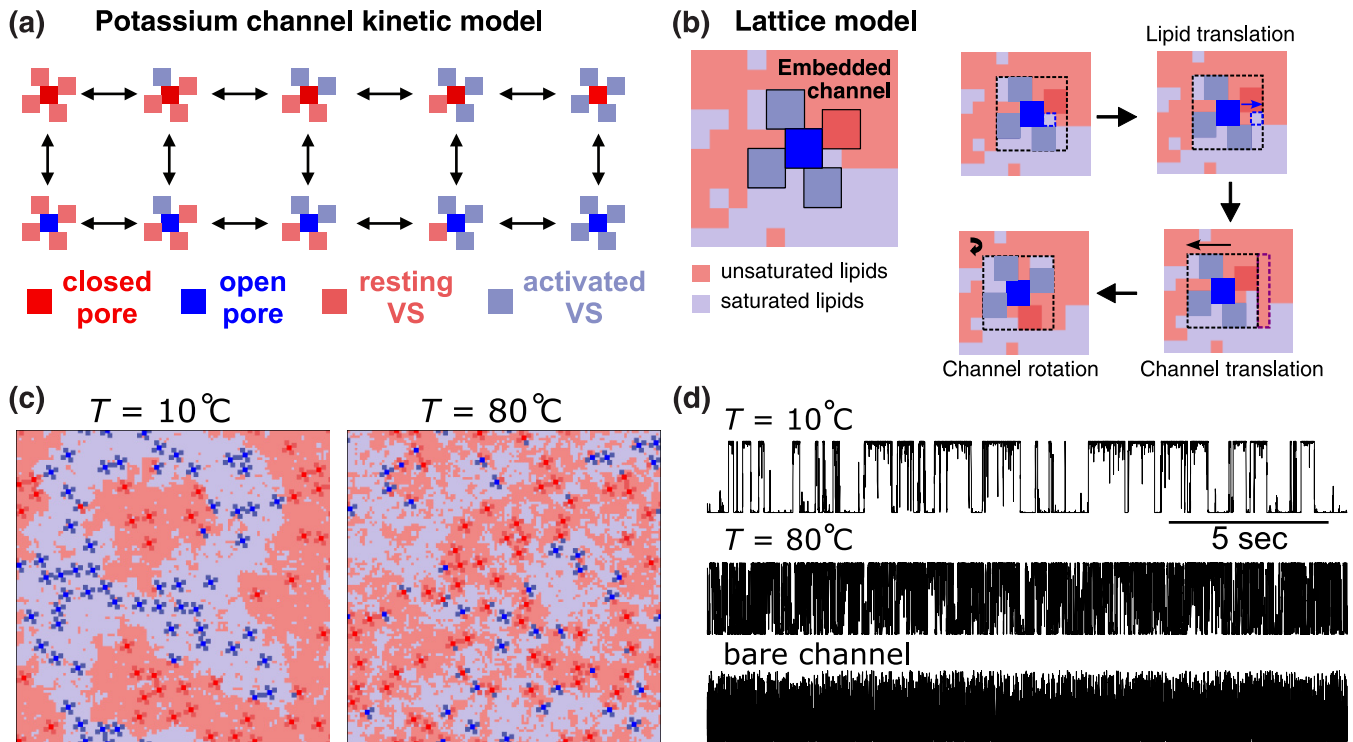


FIG. 5. (a) Ten-state activation scheme for a potassium channel. The central pore, in dark red/blue for closed/open state, is surrounded by four allosterically linked voltage sensors (VS) in light red/blue for resting/activated states. Rate constants between different states are described in the SM [29]. (b) Lattice model. The channel is embedded as (2×2) pore in contact with four symmetrically arranged (2×2) voltage sensors. The channel is surrounded by embedded lipids (lighter red/blue for unsaturated/saturated lipids) occupying each a single cell. Implemented translational and rotational degrees of freedom are shown on the right. (c) Snapshots of the lattice model at $T = 10^\circ\text{C}$, 80°C , and approximate half-activation voltage $V = 40$ mV below and above the demixing transition. (d) Conductance time course of a single embedded channel at $T = 10^\circ\text{C}$, 80°C , and bare channel kinetics at $T = 30^\circ\text{C}$.

(iii) translational diffusion coefficients of lipids and channels. The dynamics of the system were simulated using the kinetic Monte Carlo method of Gillespie [59] based on the chemical master equation whose rate constants from two states are assumed to have an Arrhenius form with a different rate coefficient for each specific Monte Carlo move. A detailed description of parameter choices and methods for computation can be found in the SM [29].

Figure 5(c) shows a snapshot of the lattice system near the midpoint of channel activation ($V = -40$ mV) at subcritical (10°C) and supercritical (80°C) temperatures. At 10°C the system is phase separated (demixed). Similar to the mesoscopic model, the activation state of a channel generally aligns with the lipid phase in which it resides. At 80°C , phases are mixed. Figure 5(d) shows a long (20-sec) single-channel tracing characterized by periods of substantially different open probabilities linked to slow transitions between different lipid phases, increasing in frequency with rising temperature. Because these phaselike transitions are slow compared to the millisecond Markovian kinetics of the isolated channel (bottom trace, at 30°C), they can be considered modal events [38,39].

1. Cooperativity and hysteresis

To test for hysteresis, we implemented a double ramp protocol with rising (ON) and falling (OFF) phases acquired at

a ramp speed of ± 0.1 mV/ms. With this slow-ramp protocol, entire (quasistatic) ON and OFF activation curves were acquired in a single 4-sec simulation. We measured the conductance Hill plots and Q - V curves of averaged activation curves from 100 embedded channels (channel density of $f_p = 7.8 \times 10^{-3}$), Figs. 6(a) and 6(b). The vertical separation of skew asymptotes in the Hill plot was used to measure the pore-voltage sensor coupling energy ΔW at $T = 10^\circ\text{C}$, for isolated (bare) and embedded channels.

The bare channel yielded overlapping ON and OFF activation curves, while Q - V hysteresis was seen with embedded channels, accompanied by temperature-sensitive cooperativity [Figs. 6(c)–6(d)]. These behaviors are consistent with the idea developed in the previous section that membrane demixing promotes channel-channel cooperativity, and hysteresis arises from the relatively long time it takes a channel to migrate between phases. Upon increasing the temperature, we again observed lessening hysteresis from the mixing of lipid phases.

2. Long-term memory and Hurst analysis

We questioned whether lipid-embedded channels can exhibit long-term memory of the type observed in single-channel records from BK channels [30–34]. This phenomenon differs from short-term memory in Markov models, in which dwell-time distributions demonstrate a finite number of

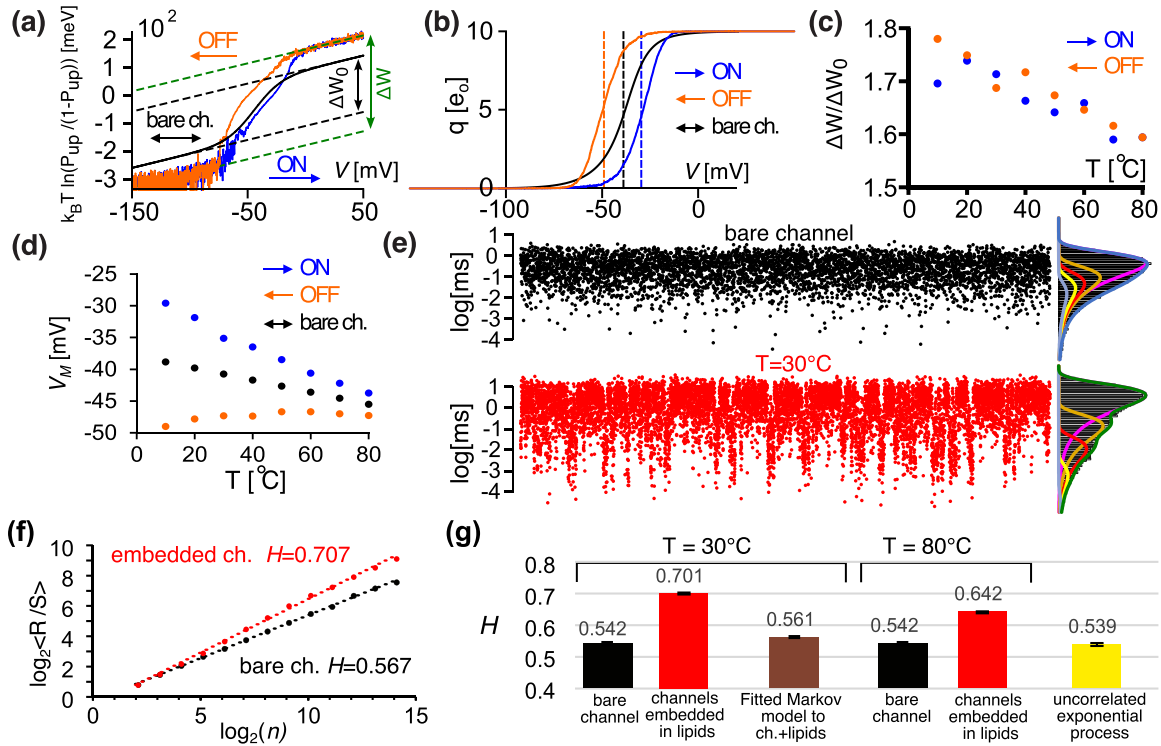


FIG. 6. (a) Hill plot for 2-sec rising ON (blue) and falling OFF (orange) voltage ramp (± 0.1 mV/ms) conductance of the embedded channel compared to the quasistatic behavior of the bare channel (black line) at $T = 10^\circ\text{C}$. Arrows indicate the ramp direction. The pore linkage energy ΔW is the vertical separation between skew asymptotes (dashed lines). Note the smaller separation ΔW_0 for the bare channel. (b) Q - V curves obtained with the same ramp protocol as in (a). The median voltages of activation V_M (values at which half of the channels are activated) are indicated by the dashed lines. (c) Ratio of ΔW to the constant value $\Delta W_0 = 200$ meV of the bare channel as a function of temperature for the ON and OFF voltage ramps. (d) V_M values for the ON and OFF ramps as a function of temperature, compared to the bare channel case. Q - V curve hysteresis decreases with temperature, as demonstrated by the convergence of the ON/OFF V_M values. (e) Sequential open dwell times for bare (black) and embedded (red) channels at $T = 30^\circ\text{C}$, $V = 40$ mV. The semilog dwell-time distributions fitted to the eigencomponents (solid lines) of the ten-state model are shown to the right of the sequences. (f) Single-channel Hurst plots comparing slopes (H) of bare (black) and embedded (red) channels at $T = 30^\circ\text{C}$. (g) Averaged ($n = 100$) Hurst exponents H for bare (black bars) and embedded (orange bars) channels at $T = 30^\circ\text{C}$, 80°C . The two control cases with exponents near 0.5 are (1) a bare channel whose Markov gating scheme was fitted to the dwell-time distribution of the embedded channel (brown bar); (2) an uncorrelated sequence of exponentially distributed dwell times (yellow bar).

exponential decays [7]. Long-term memory follows a power law characterized by self-similarity in a process $B(t)$ satisfying $B(at) \sim |a|^H B(t)$, where H is the Hurst exponent [60]. If $H > 1/2$ ($H < 1/2$), the process has long-term positive (negative) autocorrelation, while $H = 1/2$ for uncorrelated processes.

We applied Hurst analysis to consecutive open dwell times from 100 embedded channels [Fig. 6(e)]. Simulations were run under equilibrium conditions at the half-activation potential $V = -40$ mV and at temperatures $T = 30^\circ\text{C}$ and 80°C , until every channel experienced at least 2^{14} opening events. Bare channels governed by the ten-state Markov model demonstrated longitudinal homogeneity in their dwell-time sequence, whereas dwell-time sequences of embedded channels were more erratic. It was possible to fit the broadened dwell-time distribution of the embedded channel to the original ten-state Markov model by adjusting kinetic parameters. The fitted Markov model of the embedded channel was used as a control in the Hurst analysis.

We performed the standard determination of the Hurst exponent from the slope of $\log_2 R(n)/S(n)$ versus $\log_2(n)$,

averaged over subsets of data of size n , where $R(n)$ is the range of the summed deviation from the mean dwell time and $S(n)$ is the standard deviation [60]. The slope was estimated through linear regression for n ranging from 2 to 14. This method overestimates H due to sampling bias in small bins [61] but is consistent with previous analysis of experimental data [35]. In practice, determining the absence of long-term correlations was achieved by comparing to internal controls.

Typical Hurst plots and fitted exponents are shown in Figs. 6(f) and 6(g). The average Hurst exponent for the bare channel (Markov case) is equal to 0.542 ± 0.018 (mean \pm std. dev.), a result that is independent of temperature. Although H is slightly greater than 0.5, it is statistically no different from an uncorrelated series of exponential deviates ($H = 0.539 \pm 0.019$, $p = 0.24$, student's t -test), demonstrating the absence of long-term memory.

On the other hand, in embedded channels we find $H = 0.701 \pm 0.018$, consistent with outside experimental values of H in the BK channel that vary from 0.61 to 0.71 [30–32,34]. There is lipid-induced broadening of dwell-time distributions that accompanies increased H values, but this does not explain

long-term memory, as the fitted Markov model to the embedded channel distribution is near the uncorrelated value ($H = 0.561 \pm 0.016$). Increasing the temperature to 80 °C reduces but does not abolish long-term memory ($H = 0.642 \pm 0.016$), consistent with the earlier hysteresis results.

III. CONCLUSIONS

The aim of our study was to investigate the consequences of state-dependent channel affinity for different lipid species in demixing membranes. We found that when lipids are phase separated, ion channels exhibit clustering, cooperativity, hysteresis, and long-term memory effects.

In particular, we have shown that fluctuations in local lipid composition give rise to effective attractive interactions and to correlations between ion channels, even when they are far apart. These effects are responsible for the observed clustering tendency and cooperativity of activation. Moreover, since the typical relaxation times of these fluctuations is longer than any timescale involved in channel activation, the channel dynamics shows memory effects, including hysteresis of the activation curve.

The membrane influence provides explanations for previously puzzling experimental observations and generates testable predictions. In particular, fluorescence microscopy techniques could be used to measure the size distribution of clusters of ion channels for different lipid compositions to correlate cluster properties to the phase behavior of the underlying membrane. Our model predicts that the largest clustering tendency occurs for near-critical membranes with a characteristic size distribution showing a power-law tail with a precise exponent. From the point of view of electrophysiology, we expect the slope of the G - V and Q - V curves (and their hysteresis effects) to show distinct dependencies on temperature and lipid composition, reflecting the fact that critical membranes enhance cooperativity in a predictable fashion. Similarly, the hypothesis of a long-range coupling mediated by lipids could be tested by measuring the influence of channel density on the slope of the activation curve. Finally, single-channel recording experiments could be designed to characterize long-term

memory in ionic currents for different temperatures and lipid compositions.

Experimental confirmation of the paradigm proposed here would pave the way for a new class of effective models bridging membrane physics and physiology. Coupling ion-channel conformational states and local lipid composition introduces a new level of complexity to the quantitative description of channel activity by taking into account the cellular context. For instance, the activity of several members of voltage-gated ion channels family is regulated by PIP2, a signaling lipid molecule that can facilitate or inhibit channel activation [62] and that has been suggested to localize preferentially in lipid rafts [63]. The coupling between channel activation and raft formation and disruption hypothesized here could have consequences on the PIP2 local concentration dynamics and thus potentially underlie some of the complex mechanisms employed by cells to modulate membrane excitability. Although the generality of these mechanisms is not yet fully understood, it is likely that state-dependent lipid coupling plays a significant physiological role, particularly in neurons where channels are abundant and interconnected [8]. Specifically, clustering and cooperativity [37] appear to have important functional consequences [9]. Importantly, some of these mechanisms are likely at work in other types of membrane proteins with similar state-dependent affinity [23], suggesting a universal class of self-organizing biomolecular systems.

ACKNOWLEDGMENTS

This research includes calculations carried out using Temple University's HPC resources and thus was supported in part by the National Science Foundation through Major Research Instrumentation Grant No. 1625061 and by the US Army Research Laboratory under Contract No. W911NF-16-2-0189. We acknowledge funding from MIUR Projects No. PRIN 2020/PFCXPE and No. 2022/HNW5YL. V.C. is supported by the National Institute of General Medical Science of the National Institutes of Health under Award No. R01GM093290.

-
- [1] B. Katz and R. Miledi, The statistical nature of the acetylcholine potential and its molecular components, *J. Physiol.* **224**, 665 (1972).
 - [2] C. Anderson and C. Stevens, Voltage clamp analysis of acetylcholine produced end-plate current fluctuations at frog neuromuscular junction, *J. Physiol.* **235**, 655 (1973).
 - [3] A. L. Hodgkin and A. F. Huxley, A quantitative description of membrane current and its application to conduction and excitation in nerve, *J. Physiol.* **117**, 500 (1952).
 - [4] D. Colquhoun and A. G. Hawkes, The principles of the stochastic interpretation of ion-channel mechanisms, *Single-Channel Recording* (Plenum Press, New York, 1995), 397–482.
 - [5] F. J. Sigworth, Voltage gating of ion channels, *Q. Rev. Biophys.* **27**, 1 (1994).
 - [6] F. Bezanilla, Gating currents, *J. Gen. Physiol.* **150**, 911 (2018).
 - [7] C. Shelley, X. Niu, Y. Geng, and K. L. Magleby, Coupling and cooperativity in voltage activation of a limited-state BK channel gating in saturating Ca^{2+} , *J. Gen. Physiol.* **135**, 461 (2010).
 - [8] D. Sato, G. Hernández-Hernández, C. Matsumoto, S. Tajada, C. M. Moreno, R. E. Dixon, S. O'Dwyer, M. F. Navedo, J. S. Trimmer, C. E. Clancy *et al.*, A stochastic model of ion channel cluster formation in the plasma membrane, *J. Gen. Physiol.* **151**, 1116 (2019).
 - [9] P. Pfeiffer, A. V. Egorov, F. Lorenz, J.-H. Schleimer, A. Draguhn, and S. Schreiber, Clusters of cooperative ion channels enable a membrane-potential-based mechanism for short-term memory, *eLife* **9**, e49974 (2020).
 - [10] N. C. Vierra, S. C. O'Dwyer, C. Matsumoto, L. F. Santana, and J. S. Trimmer, Regulation of neuronal excitation–transcription coupling by Kv2.1-induced clustering of somatic L-type Ca^{2+}

- channels at ER-PM junctions, *Proc. Natl. Acad. Sci.* **118**, e2110094118 (2021).
- [11] C. M. Moreno, R. E. Dixon, S. Tajada, C. Yuan, X. Opitz-Araya, M. D. Binder, and L. F. Santana, Ca^{2+} entry into neurons is facilitated by cooperative gating of clustered $\text{CaV}1.3$ channels, *eLife* **5**, e15744 (2016).
- [12] B. F. Lillemeier, J. R. Pfeiffer, Z. Surviladze, B. S. Wilson, and M. M. Davis, Plasma membrane-associated proteins are clustered into islands attached to the cytoskeleton, *Proc. Natl. Acad. Sci. USA* **103**, 18992 (2006).
- [13] Y. Liu and J. P. Dilger, Application of the one-and two-dimensional Ising models to studies of cooperativity between ion channels, *Biophys. J.* **64**, 26 (1993).
- [14] H. M. Seeger, L. Aldrovandi, A. Alessandrini, and P. Facci, Changes in single K^+ channel behavior induced by a lipid phase transition, *Biophys. J.* **99**, 3675 (2010).
- [15] B. B. Machta, S. L. Veatch, and J. P. Sethna, Critical Casimir forces in cellular membranes, *Phys. Rev. Lett.* **109**, 138101 (2012).
- [16] R. K. Hite, J. A. Butterwick, and R. MacKinnon, Phosphatidic acid modulation of Kv channel voltage sensor function, *eLife* **3**, e04366 (2014).
- [17] S. Katira, K. K. Mandadapu, S. Vaikuntanathan, B. Smit, and D. Chandler, Pre-transition effects mediate forces of assembly between transmembrane proteins, *eLife* **5**, e13150 (2016).
- [18] O. Kimchi, S. L. Veatch, and B. B. Machta, Ion channels can be allosterically regulated by membrane domains near a de-mixing critical point, *J. Gen. Physiol.* **150**, 1769 (2018).
- [19] A. L. Duncan, W. Song, and M. S. P. Sansom, Lipid-dependent regulation of ion channels and G protein-coupled receptors: Insights from structures and simulations, *Annu. Rev. Pharmacol. Toxicol.* **60**, 31 (2020).
- [20] A. L. Duncan, R. A. Corey, and M. S. P. Sansom, Defining how multiple lipid species interact with inward rectifier potassium (Kir2) channels, *Proc. Natl. Acad. Sci.* **117**, 7803 (2020).
- [21] J. Bodosa, S. S. Iyer, and A. Srivastava, Preferential protein partitioning in biological membrane with coexisting liquid ordered and liquid disordered phase behavior: Underlying design principles, *J. Membr. Biol.* **253**, 551 (2020).
- [22] V. Shiva Mandala and R. MacKinnon, Voltage-sensor movements in the Eag Kv channel under an applied electric field, *Proc. Natl. Acad. Sci.* **119**, e2214151119 (2022).
- [23] I. Levental and E. Lyman, Regulation of membrane protein structure and function by their lipid nano-environment, *Nat. Rev. Mol. Cell Biol.* **24**, 107 (2022).
- [24] S. L. Veatch and S. L. Keller, Separation of liquid phases in giant vesicles of ternary mixtures of phospholipids and cholesterol, *Biophys. J.* **85**, 3074 (2003).
- [25] E. Sezgin, I. Levental, S. Mayor, and C. Eggeling, The mystery of membrane organization: Composition, regulation and roles of lipid rafts, *Nat. Rev. Mol. Cell Biol.* **18**, 361 (2017).
- [26] T. R. Shaw, S. Ghosh, and S. L. Veatch, Critical phenomena in plasma membrane organization and function, *Annu. Rev. Phys. Chem.* **72**, 51 (2021).
- [27] G. A. Pantelopulos and J. E. Straub, Regimes of complex lipid bilayer phases induced by cholesterol concentration in MD simulation, *Biophys. J.* **115**, 2167 (2018).
- [28] A. R. Honerkamp-Smith, S. L. Veatch, and S. L. Keller, An introduction to critical points for biophysicists; Observations of compositional heterogeneity in lipid membranes, *Biochim. Biophys. Acta, Biomembr.* **1788**, 53 (2009).
- [29] See Supplemental Material at <http://link.aps.org/supplemental/10.1103/PRXLife.2.013007> for the model details and additional analysis, which includes Refs. [64–80].
- [30] W. A. Varanda, L. S. Liebovitch, J. N. Figueiroa, and R. A. Nogueira, Hurst analysis applied to the study of single calcium-activated potassium channel kinetics, *J. Theor. Biol.* **206**, 343 (2000).
- [31] Z. Siwy, S. Mercik, K. Weron, and M. Ausloos, Application of dwell-time series in studies of long-range correlation in single channel ion transport: Analysis of ion current through a big conductance locust potassium channel, *Physica A* **297**, 79 (2001).
- [32] H. T. Bandeira, C. T. F. Barbosa, R. A. Campos de Oliveira, J. F. Aguiar, and R. A. Nogueira, Chaotic model and memory in single calcium-activated potassium channel kinetics, *Chaos: An Interdisciplinary Journal of Nonlinear Science* **18**, 033136 (2008).
- [33] A. Wawrzkiwicz-Jałowicka, B. Dworakowska, and Z. J. Grzywna, The temperature dependence of the BK channel activity-kinetics, thermodynamics, and long-range correlations, *Biochim. Biophys. Acta, Biomembr.* **1859**, 1805 (2017).
- [34] A. Wawrzkiwicz-Jałowicka, P. Trybek, Ł. Machura, B. Dworakowska, and Z. J. Grzywna, Mechanosensitivity of the BK channels in human glioblastoma cells: Kinetics and dynamical complexity, *J. Membr. Biol.* **251**, 667 (2018).
- [35] M. P. Silva, C. G. Rodrigues, W. A. Varanda, and R. A. Nogueira, Memory in ion channel kinetics, *Acta Biotheor.* **69**, 697 (2021).
- [36] É. Faure, C. Thompson, and R. Blunck, Do lipids show state-dependent affinity to the voltage-gated potassium channel KvAP? *J. Biol. Chem.* **289**, 16452 (2014).
- [37] R. E. Dixon, M. F. Navedo, M. D. Binder, and L. F. Santana, Mechanisms and physiological implications of cooperative gating of clustered ion channels, *Physiol. Rev.* **102**, 1159 (2022).
- [38] J. B. Patlak, K. A. F. Gration, and P. N. R. Usherwood, Single glutamate-activated channels in locust muscle, *Nature (London)* **278**, 643 (1979).
- [39] K. L. Magleby and B. S. Pallotta, Burst kinetics of single calcium-activated potassium channels in cultured rat muscle, *J. Physiol.* **344**, 605 (1983).
- [40] I. Siekmann, J. Sneyd, and E. J. Crampin, Statistical analysis of modal gating in ion channels, *Proc. R. Soc. London A* **470**, 20140030 (2014).
- [41] F. Bezanilla and C. A. Villalba-Galea, The gating charge should not be estimated by fitting a two-state model to a QV curve, *J. Gen. Physiol.* **142**, 575 (2013).
- [42] J. Cowgill and B. Chanda, Charge-voltage curves of shaker potassium channel are not hysteretic at steady state, *J. Gen. Physiol.* **155**, e202112883 (2023).
- [43] C. A. Villalba-Galea and A. T. Chiem, Hysteretic behavior in voltage-gated channels, *Front. Pharmacol.* **11**, 579596 (2020).
- [44] S. L. Veatch and S. L. Keller, Seeing spots: Complex phase behavior in simple membranes, *Biochim. Biophys. Acta, Mol. Cell Res.* **1746**, 172 (2005).
- [45] A. J. García-Sáez, S. Chiantia, and P. Schuille, Effect of line tension on the lateral organization of lipid membranes, *J. Biol. Chem.* **282**, 33537 (2007).

- [46] M. Javanainen, H. Martinez-Seara, and I. Vattulainen, Nanoscale membrane domain formation driven by cholesterol, *Sci. Rep.* **7**, 1143 (2017).
- [47] R.-X. Gu, S. Baoukina, and D. P. Tieleman, Phase separation in atomistic simulations of model membranes, *J. Am. Chem. Soc.* **142**, 2844 (2020).
- [48] Q. Novinger, A. Suma, D. Sigg, G. Gonnella, and V. Carnevale, Particle-based Ising model, *Phys. Rev. E* **103**, 012125 (2021).
- [49] H. E. Stanley, Scaling, universality, and renormalization: Three pillars of modern critical phenomena, *Rev. Mod. Phys.* **71**, S358 (1999).
- [50] A. Bandara, A. Panahi, G. A. Pantelopulos, T. Nagai, and J. E. Straub, Exploring the impact of proteins on the line tension of a phase-separating ternary lipid mixture, *J. Chem. Phys.* **150**, 204702 (2019).
- [51] B. J. Reynwar and M. Deserno, Membrane composition-mediated protein-protein interactions, *Biointerphases* **3**, FA117 (2008).
- [52] D. Stauffer and A. Aharony, *Introduction to Percolation Theory* (Taylor & Francis, London, 2018).
- [53] D. Sigg, A linkage analysis toolkit for studying allosteric networks in ion channels, *J. Gen. Physiol.* **141**, 29 (2013).
- [54] A. Paraschiv, S. Hegde, R. Ganti, T. Pilizota, and A. Šarić, Dynamic clustering regulates activity of mechanosensitive membrane channels, *Phys. Rev. Lett.* **124**, 048102 (2020).
- [55] O. B. McManus, D. S. Weiss, C. E. Spivak, A. L. Blatz, and K. L. Magleby, Fractal models are inadequate for the kinetics of four different ion channels, *Biophys. J.* **54**, 859 (1988).
- [56] D. H. Cox, J. Cui, and R. W. Aldrich, Allosteric gating of a large conductance Ca-activated K⁺ channel, *J. Gen. Physiol.* **110**, 257 (1997).
- [57] F. T. Horrigan and R. W. Aldrich, Allosteric voltage gating of potassium channels II: Mslo channel gating charge movement in the absence of Ca²⁺, *J. Gen. Physiol.* **114**, 305 (1999).
- [58] F. T. Horrigan and R. W. Aldrich, Coupling between voltage sensor activation, Ca²⁺ binding and channel opening in large conductance (BK) potassium channels, *J. Gen. Physiol.* **120**, 267 (2002).
- [59] D. T. Gillespie, Exact stochastic simulation of coupled chemical reactions, *J. Phys. Chem.* **81**, 2340 (1977).
- [60] J. Beran, *Statistics for Long-Memory Processes* (CRC Press, Boca Raton, FL, 1994), Vol. 61.
- [61] J. B. Basingthwaight and G. M. Raymond, Evaluating rescaled range analysis for time series, *Ann. Biomed. Eng.* **22**, 432 (1994).
- [62] E. J. Dickson and B. Hille, Understanding phosphoinositides: Rare, dynamic, and essential membrane phospholipids, *Biochem. J.* **476**, 1 (2019).
- [63] J. Myeong, C.-G. Park, B.-C. Suh, and B. Hille, Compartmentalization of phosphatidylinositol 4, 5-bisphosphate metabolism into plasma membrane liquid-ordered/raft domains, *Proc. Natl. Acad. Sci.* **118**, e2025343118 (2021).
- [64] A. Coniglio and A. Fierro, Correlated percolation, in *Encyclopedia of Complexity and Systems Science*, edited by R. A. Meyers (Springer, New York, 2009), pp. 1596–1615.
- [65] A. Clauset, C. Rohilla Shalizi, and M. E. J. Newman, Power-law distributions in empirical data, *SIAM Rev.* **51**, 661 (2009).
- [66] W. Shinoda, M. Shiga, and M. Mikami, Rapid estimation of elastic constants by molecular dynamics simulation under constant stress, *Phys. Rev. B* **69**, 134103 (2004).
- [67] A. P. Thompson, H. M. Aktulga, R. Berger, D. S. Bolintineanu, W. M. Brown, P. S. Crozier, P. J. in 't Veld, A. Kohlmeyer, S. G. Moore, T. D. Nguyen, R. Shan, M. J. Stevens, J. Tranchida, C. Trott, and S. J. Plimpton, LAMMPS - A flexible simulation tool for particle-based materials modeling at the atomic, meso, and continuum scales, *Comput. Phys. Commun.* **271**, 108171 (2022).
- [68] G. Kemmer and S. Keller, Nonlinear least-squares data fitting in excel spreadsheets, *Nat. Protoc.* **5**, 267 (2010).
- [69] D. Colquhoun and A. G. Hawkes, *A Q-Matrix Cookbook* (Springer, New York, 1995), pp. 589–633.
- [70] E. Stefani, L. Toro, E. Perozo, and F. Bezanilla, Gating of shaker K⁺ channels: I. Ionic and gating currents, *Biophys. J.* **66**, 996 (1994).
- [71] W. N. Zagotta, T. Hoshi, and R. W. Aldrich, Shaker potassium channel gating. III: Evaluation of kinetic models for activation, *J. Gen. Physiol.* **103**, 321 (1994).
- [72] E. N. Senning and S. E. Gordon, Activity and Ca²⁺ regulate the mobility of TRPV1 channels in the plasma membrane of sensory neurons, *eLife* **4**, e03819 (2015).
- [73] R. Peters and R. J. Cherry, Lateral and rotational diffusion of bacteriorhodopsin in lipid bilayers: Experimental test of the Saffman-Delbrück equations. *Proc. Natl. Acad. Sci. USA* **79**, 4317 (1982).
- [74] A. I. Fernández-Mariño, X.-F. Tan, C. Bae, K. Huffer, J. Jiang, and K. J. Swartz, Inactivation of the Kv2.1 channel through electromechanical coupling, *Nature (London)* **622**, 410 (2023).
- [75] A. N. Leonard and E. Lyman, Activation of G-protein-coupled receptors is thermodynamically linked to lipid solvation, *Biophys. J.* **120**, 1777 (2021).
- [76] S. Chowdhury and B. Chanda, Estimating the voltage-dependent free energy change of ion channels using the median voltage for activation, *J. Gen. Physiol.* **139**, 3 (2012).
- [77] S. Chowdhury and B. Chanda, Deconstructing thermodynamic parameters of a coupled system from site-specific observables, *Proc. Natl. Acad. Sci.* **107**, 18856 (2010).
- [78] D. T. Gillespie, Stochastic simulation of chemical kinetics, *Annu. Rev. Phys. Chem.* **58**, 35 (2007).
- [79] D. Sigg and F. Bezanilla, Total charge movement per channel. the relation between gating charge displacement and the voltage sensitivity of activation, *J. Gen. Physiol.* **109**, 27 (1997).
- [80] D. Sigg, H. Qian, and F. Bezanilla, Kramers' diffusion theory applied to gating kinetics of voltage-dependent ion channels, *Biophys. J.* **76**, 782 (1999).